ACS AuthorChoice

Environmental Science & Technology

Article

pubs.acs.org/est

Terms of Use

Effect of pH and Stream Order on Iron and Arsenic Speciation in Boreal Catchments

Elisabeth Neubauer,[†] Stephan J. Köhler,[‡] Frank von der Kammer,*[,†] Hjalmar Laudon,[§] and Thilo Hofmann*[,†]

[†]Department of Environmental Geosciences, University of Vienna, Althanstraße 14, 1090 Vienna, Austria

[‡]Department of Aquatic Sciences and Assessment, Swedish University of Agricultural Sciences, P.O. Box 7050, SE-750 07 Uppsala, Sweden

[§]Department of Forest Ecology and Management, Swedish University of Agricultural Sciences, SE-901 83 Umeå, Sweden

Supporting Information

ABSTRACT: Riverine transport of iron (Fe) and arsenic (As) is affected by their associations with natural organic matter (NOM) and suspended iron (oxy)hydroxides. Speciation has a strong influence on element transport from the headwaters to the ocean because NOM may be transported over longer distances compared to iron (oxy)hydroxides. We show that Fe speciation changes along the flow path of a boreal watercourse, as water moves from NOM-rich, acidic first-order streams with pH as low as 3.9 to less acidic higher-order systems (up to pH 6.4). Analysis by Flow Field-Flow Fractionation and chemical equilibrium modeling revealed that Fe from wetland-dominated headwaters was mainly exported as Fe-NOM complexes; in catchments with a stream order >1 and with higher pH, Fe was present in Fe-NOM complexes and precipitated as nanoparticulate iron(oxy)hydroxides which aggregated as the pH increased, with their size eventually exceeding the membrane filters cutoff (0.2 μm). The measured NOM-bound Fe decreased with increasing pH, from 0.38 to 0.16 mmol Fe·g_{NOM}^{-1}. The high concentrations of NOM-bound Fe emphasize the importance of boreal catchments to Fe export to the oceans. Concentrations of As in the <0.2 μm fraction but larger than what is usually considered "truly dissolved" (<1000 g·mol^{-1}), decreased from 75% to 26% with increasing pH. The As in this size range was mainly associated with NOM but at pH >4.5 became associated with iron(oxy)hydroxides, and its transport thus became more coupled to that of the iron(oxy)hydroxides downstream in the circumneutral streams.

INTRODUCTION

Boreal rivers transport large quantities of natural organic matter (NOM) and associated micronutrients, such as iron (Fe) and trace elements, to the oceans.[1,2] The speciation of Fe in rivers draining into oceans has recently received an increasing amount of attention, in particular with regard to comparing the distribution of Fe-NOM complexes with that of suspended iron (oxy)hydroxides.[3−5]

In estuarine mixing zones, the solubility of organically bound elements is strongly affected by increases in ionic strength and concentration of inorganic ligands.[4] However, mixing experiments of freshwater samples containing Fe-NOM complexes and iron (oxy)hydroxides with seawater have shown that iron (oxy)hydroxides are more likely to aggregate and settle than Fe-NOM complexes[3,4] and Fe-NOM complexes are therefore considered to be transported over longer distances.[4] NOM concentrations in many boreal catchments have been increasing over recent decades due to changes in atmospheric deposition of sulfate and changing hydrological flow conditions.[1,6] This has led to an increase in Fe concentrations in the boreal zone and the browning of surface water.[7]

Most studies investigating the behavior of NOM, suspended iron (oxy)hydroxides, and associated trace elements, have been carried out in large streams with little consideration given to how the water chemistry evolves during its transit within the drainage network. Important processes may however also occur along the flow path of a watercourse, i.e., as water moves from more acidic first-order streams to less acidic higher-order systems,[8] and affect the mobilization of Fe and NOM and Fe speciation. NOM from different sources within a catchment area can exhibit different metal binding properties.[9,10] The distribution of soil types such as wetland soils and forested soils[11] may therefore influence the export of Fe-NOM

Received: March 18, 2013
Revised: May 16, 2013
Accepted: May 21, 2013
Published: May 21, 2013

 © 2013 American Chemical Society

complexes. Iron (oxy)hydroxides can precipitate in riparian zones, where Fe-rich anoxic groundwater flows into a stream.[12] Fe(III) that was previously bound to NOM can also precipitate as iron (oxy)hydroxides when the pH of the water increases due to the strong hydrolytic tendency of Fe(III).[13] In-stream iron (oxy)hydroxide growth and agglomeration then results in larger particles that settle out in the slow-flowing sections of streams, lakes, or estuaries, affecting the fate of many metals and metalloids such as lead (Pb), chromium (Cr), and arsenic oxyanions (As) that are bound to the iron (oxy)hydroxides. The extent to where and how fast this process occurs within a stream network is not well studied.

Iron (oxy)hydroxides act as one of the most important controls affecting the distribution of As between dissolved and solid phases, due to the high affinity of As for iron (oxy)hydroxides under oxic conditions.[14,15] The speciation of Fe is therefore of particular importance when quantifying fluxes of As in rivers.[16] As can, however, also be complexed by NOM.[17,18] The formation of ternary complexes, with Fe acting as a cation bridge,[19,20] may enhance As binding to NOM.[20] Arsenic speciation is therefore likely to be greatly influenced by whether Fe is present as Fe-NOM complexes or as iron (oxy)hydroxides.[13]

The objectives of this study were (i) to investigate sources of NOM, As, and Fe in a boreal catchment as the water moves from small, acidic, wetland and forest dominated catchments (covering 0.03−0.7 km^2) to less acidic higher-order streams with larger catchment areas (up to 70 km^2), (ii) to quantify and model organically bound Fe in order to improve our understanding of Fe and NOM mobilization in boreal landscapes, and (iii) to identify how the processes controlling Fe speciation (i.e., the formation of Fe-NOM complexes and iron (oxy)hydroxides) affect the transport of NOM-associated As. Flow-Field Flow Fractionation (FlowFFF) coupled to inductively coupled plasma mass spectrometry (ICP-MS) was used to invesigate Fe and As association with NOM.

MATERIALS AND METHODS

Site Description. The investigated catchment (the Krycklan River catchment, Sweden: 64°14′N, 19°46′E) comprises a network of streams ranging from first-order headwater streams to fourth-order boreal streams, with the catchment areas of these subdrainages ranging from 0.03 km^2 to 67 km^2 (Figure S1). There is a high spatial variability in pH across the catchment, with baseflow pH ranging from 3.9 to 6.5 at the various locations.[21] The pH generally increases with increasing flowpath length due to decreasing NOM concentrations and increasing HCO_3^- concentrations and is therefore higher in the larger downstreams rivers[21] (Table 1, Table S2). The Krycklan River is a tributary to the Vindelälven River, which flows into the Baltic Sea near Umeå. Fourteen of its subcatchments (hereafter referred to as C1−C16) were sampled. The bedrock consists of Svecofennian rocks comprising mainly metasediments or metagreywackes.[22] The cover of glacial till in the upper part of the catchment gives way to sorted sediments in the lower parts of the catchment, consisting mainly of sand and silt (Figure S1).[22] Most of the upslope parts of the catchments are covered by podzols, while organic-rich soils are common in the riparian zones.[21] The upslope areas are mainly forested with Scots Pine (*Pinus sylvestris*) and the low lying areas with Norway Spruce (*Picea abies*).[21] The forested landscape is interspersed with patches of sphagnum-dominated peat wetlands (Figure S1). The C1 and C2 locations are first-order streams that drain forested catchments, with a forest coverage of >98%, while sites C3 and C4 drain wetlands (40−76% wetland coverage), and C5 is the outlet of a lake (Table 1).[22] The other sites are mixed catchments which are covered by forests (73 to 89%), wetlands (8 to 26%), and lakes and arable land (<4%).[22]

Table 1. Stream Order, Area, Landscape Type, pH, and DOC Concentrations of the Stream Sampling Sites

site	stream order	area (km^2)	landscape type	pH	DOC ($mg{\cdot}L^{-1}$)
C1	1	0.66	forested	5.1	27.2
C2	1	0.13	forested	4.6	26.4
C3	1	0.03	wetland	3.9	53.3
C4	1	0.19	wetland	4.1	43.7
C5	1	0.95	lake outlet	4.7	25.5
C6	1	1.40	mixed	5.0	23.6
C7	2	0.50	mixed	4.5	34.6
C9	2	3.14	mixed	5.3	23.2
C10	2	2.94	mixed	4.6	31.2
C12	2	5.40	mixed	4.9	29.2
C13	3	7.21	mixed	5.2	27.4
C14	3	13.6	mixed	6.2	18.6
C15	4	19.9	mixed	6.3	20.5
C16	4	67.8	mixed	6.4	19.6

Sampling and in Situ Measurements. The water level at site C7 was recorded using a 90° V-notch weir in a dam house, and discharge was calculated using established height-discharge rating curves.[21] Samples were collected in September 2011, at the end of the growing season when biological activity starts to decline, during moderate to high flow conditions (1.0 $mm{\cdot}day^{-1}$ at site C7) a week after high rainfall and high flow rates (up to 9.7 $mm{\cdot}day^{-1}$ at site C7). The timing of the sampling was chosen to avoid both the baseflow and the highest flow conditions. This ensured a good connectivity between the streams and the groundwater aquifer and avoided the flushing of the whole system that occurs during the highest flow conditions, such as during spring flood.[22] Björkvald et al.[22] showed that the temporal variation of Fe concentrations is related to varying hydrological pathways, i.e. during high and low flow. Stream water was collected from each site using a 1L PE bottle. Water temperatures were measured *in situ* (9 to 11 °C). Dissolved oxygen concentrations were ranging between 9 and 10 $mg{\cdot}L^{-1}$. The samples were transported in closed PE bottles directly to the laboratory.

Bulk Analyses. The pH and electrical conductivity were determined using an automated titrator with a temperature-controlled (20 °C) flow-through cell (Mettler Toledo, Vienna, Austria). Fe(II) was quantified photometrically at a wavelength (λ) of 540 nm following chelation with ferrozine[23] in samples that had been filtered (<0.2 μm) and stabilized (1 M HCl) in the field (limit of quantification, LOQ: 50 $\mu g{\cdot}L^{-1}$). An aliquot of 750 mL from each sample was filtered in the laboratory within 12 h of sampling (Nalgene filter units equipped with 0.2 μm cellulose acetate filters, Sartorius Stedim, Sartorius, Göttingen, Germany). Ultrapure water was filtered and measured as blanks to ensure that no metals were leaching from the filters (Fe and As were below the LOQ in the blanks). Samples for cation determination (filtered and unfiltered) were acidified with 2% HNO_3 (Merck Suprapur grade, 65%, Merck, Darmstadt, Germany) immediately after bottling and were microwave-digested within 1 week. In summary, 20 mL from each sample was digested with 5 mL of 65% HNO_3 (Merck

dx.doi.org/10.1021/es401193j | Environ. Sci. Technol. 2013, 47, 7120−7128

Suprapur grade, Merck, Darmstadt, Germany) and 1 mL of H_2O_2 (Merck Suprapur grade, Merck, Darmstadt, Germany) in a microwave oven (Microwave 3000, Anton Paar, Graz, Austria) for 15 min at 175 °C. The digested sample was then diluted up to 100 mL with ultrapure water and stored in 100 mL PE bottles until analysis by ICP-OES (Optima 5300 DV, Perkin-Elmer, Waltham, US) and ICP-MS (7700x, Agilent Technologies, Waldbronn, Germany; LOQ Fe: 10 $\mu g \cdot L^{-1}$, LOQ As: 10 $ng \cdot L^{-1}$). Total organic carbon (TOC) and dissolved organic carbon (DOC) measurements for both unfiltered and filtered samples were collected using a TOC-5000 Analyzer (Shimadzu, Duisburg, Germany; blank 0.6 $mg \cdot L^{-1}$, precision 3%). The absorbance spectra of filtered samples were recorded for wavelengths between 230 and 550 nm, in 1 cm cuvettes (Varian Cary 50 UV−vis spectrophotometer, Varian Inc., Palo Alto, USA). The specific UV absorbance (SUVA) was calculated as the absorbance at 254 nm, divided by the DOC concentration and multiplied by 100. The aromaticity percentage of the organic matter was calculated from the SUVA (aromaticity = 6.52 · SUVA + 3.63).[24] Anions were measured using ion chromatography (ICS-1000, Dionex, Vienna, Austria; LOQ: 0.1 $mg \cdot L^{-1}$). Alkalinity of the samples with a pH >4.5 was determined within 24 h of sampling by titrating approximately 50 mg of sample with 0.002 M HCl to pH 4.5.

Humic Acid Separation. Humic acids were separated from fulvic acids and small organic acids on the basis of their pH-dependent coagulation.[25] Filtered samples (0.2 μm) were adjusted to pH <2, and the precipitated humic acids were removed by filtering over 0.2 μm cellulose acetate filters (Sartorius Stedim, Sartorius, Göttingen, Germany); the DOC concentration in the filtrate (fulvic acids and small organic molecules) was then analyzed (TOC-VCPH total organic carbon analyzer, Shimadzu, Duisburg, Germany); the precision of this method was 6%.

Binding Sites and Functional Group Titration. Column separations were used to determine the available binding sites on the DOC. Approximately 25 mL of the filtered (0.2 μm) samples were passed at constant flow through a proton saturated Dowex-50 cation exchanger column. During the passage, metals that are not bound to organic matter will exchange for protons and remain in the column. Dissolved inorganic anions (SO_4^{2-}, F^-, Cl^-, and NO_3^-), cations (Fe, Al, and Mn), and DOC were determined from the eluate. Functional group titration and analyses of site densities were performed on the eluates; the error of the site density determinations was <10%.[9] The measured DOC concentration and the concentration of inorganic anions for each sample were then used to calculate the concentration of readily reactive carboxylic groups per mg carbon. The concentrations of organic acids ($RCOO^-$) and the charge densities of NOM were calculated from site densities, DOC, and pH using a triprotic organic acid model described in detail elsewhere.[9]

Ultrafiltration. About 38 mL of each of the 0.2 μm filtered samples were ultrafiltered under nitrogen pressure, using a stirred ultrafiltration cell equipped with a regenerated cellulose filter (nominal molecular mass cutoff of 1000 $g \cdot mol^{-1}$, both Merck Millipore, Billerica, USA). The first 2 mL were discarded. A volume of 20 mL was used for organic carbon measurement (DOC-UF, Sievers 900 Portable Total Organic Carbon analyzer, GE Analytical Instruments, Manchester, UK), and 15 mL was acidified with 0.4 mL of 65% HNO_3 (Suprapur grade, Merck, Darmstadt, Germany) and used for ICP-OES and ICP-MS measurements. Several blanks were prepared using ultrapure water and following the sample procedure and then analyzed to evaluate leaching of Fe and As from the membrane. The Fe and As concentrations of the blanks were always below the LOQ. At the end of the experiment and before discarding the filter, the intactness of the membrane was tested with dextrane blue solution (molecular mass 2,000,000 $g \cdot mol^{-1}$); a passage of dextrane blue through the membrane was never observed.

FlowFFF-UV−vis-Fluorescence-ICP-MS. In the FlowFFF analysis we used a method that allows the fractionation and sizing of NOM and the quantification of associated elements.[5,26] In brief, the separation takes place in a thin (0.75 mm in this instance) channel with a flow field applied perpendicular to the main parabolic flow of a mobile phase. In Brownian mode separation the retention of particles in the channel is determined by their diffusion coefficients and consequently by their size and molecular mass.[27] The fractionation system used was an Eclipse 3+ Asymmetric Flow-Field Flow Fractionation system, with a short channel and equipped with a 300 $g \cdot mol^{-1}$ nominal molecular mass cutoff membrane (all Wyatt Technology, Dernbach, Germany). An ultraviolet/visible diode array detector (UV-DAD, Agilent Technologies 1200 series, Waldbronn, Germany; absorption wavelength selected at 254 nm) was used for the detection of colored NOM, and an ICP-MS (Agilent Technologies 7700x, Waldbronn, Germany) was coupled to the outlet of the UV-DAD detector. In addition, a fluorescence detector (Agilent Technologies 1200 Series FLD) with an excitation wavelength of 250 nm and an emission wavelength set to 410 nm was used. We used 15 mM ammonium carbonate (adjusted to pH 7 with HNO_3) as the mobile phase for the samples. In a previous study[28] we demonstrated that the Fe speciation does not change significantly during the FlowFFF analysis even though the mobile phase differs from the sample pH. This is related to the marked dilution of the sample during FlowFFF analysis and the short equilibration time (2 min) during the focusing step. Using a mobile phase with a pH of 4 is not possible because the nanoparticle recovery decreases dramatically. Calibration with polystyrene sulfonate molecular mass standards was performed at a higher ionic strength (50 mM) and is described in detail elsewhere.[26] Limits of detection for Fe and As, for the coupled FlowFFF and ICP-MS, were calculated as three times the standard deviation of a blank run (10 mL) before each sample run. The detection limit for Fe was 5.3 ± 3.1 $nmol \cdot L^{-1}$ and for As 0.13 ± 0.02 $nmol \cdot L^{-1}$. Fe and As concentrations (<0.2 μm) that were measured through the FlowFFF system were compared to bulk measurements made without passage through the FlowFFF system, providing an indication of losses (e.g., due to sorption onto tubing and the membrane: Figure S6). The deviations between the measurements by the FlowFFF system and the bulk measurements was approximately 20% for As and 30% for Fe (Figure S6 b and c). Elements coeluting with the NOM are interpreted as being complexed by NOM.[29,30] The possibility remains that iron (oxy)hydroxides with dimensions of <10 nm[30] are coeluted with the NOM.

Scanning Electron Microscopy. Scanning electron microscopy images (SEM, FEI Quanta 3D FEG instrument from FEI Company, Hilsboro, USA) were taken of the particulate material (>0.2 μm) that was deposited on the 0.2 μm membranes during filtration of the water samples. Energy dispersive X-ray spectroscopy was also performed to assess the

elemental composition of the particles (EDS on FEI-Quanta 3D FEG).

Modeling. Geochemical equilibrium modeling (Visual Minteq, version 3.0) was used to assess the concentrations of iron (oxy)hydroxide bound, NOM-bound, and truly dissolved Fe as well as the binding of As to $Fe(OH)_3$. Fe was entered as Fe(III) and was allowed to precipitate when exceeding the solubility product of ferrihydrite ($Fe(OH)_3$, with solubility product values (log K_s) of 2.69 at 25 °C and 3.61 at 10 °C).[31] Modeling of NOM was performed using the Stockholm Humic Model.[32] To describe proton and metal binding we used generic parameters for fulvic acid, as described elsewhere.[31] Modeling was performed at 10 °C and at 25 °C. To describe arsenic binding to ferrihydrite, we used the hydrous ferric oxide (HFO) model.[33]

Long-Term Averages of Streamwater Concentrations and Soil Water Sampling. Between 2003 and 2008, streamwater samples were collected as grab samples on at least a monthly basis (Figure S1).[34] The samples were analyzed for Fe and TOC using standard procedures that are described in detail in Björkvald et al.[22] Laudon et al.[34] demonstrated that the particulate fraction (>0.45 μm) of the TOC makes up, on average, less than 0.6% of the TOC throughout the catchment area. In addition to the stream sampling sites, thirteen riparian sampling sites are distributed across the catchment area (Figure S1) each equipped with ceramic cup suctions lysimeters (pore size 1 ± 0.1 μm) at 5 different soil depths (15−75 cm) within a distance of about 2 m of the corresponding stream.[35] Soil water samples were collected manually from suction lysimeters on 8 separate occasions during the summer and autumn periods of 2008 and 2009; detailed descriptions of the sampling and analysis can be found elsewhere.[11,35]

RESULTS AND DISCUSSION

DOC Variations with Flow Path and Landscape Type. DOC concentrations ranged from 53 mg·L^{-1} in the small (<1 km^2), wetland-dominated catchments to 19.6 mg·L^{-1} at the catchment outlet (Figure 1a). These concentrations are in the range of other wetland draining catchments in the boreal region.[12,36,37] The pH generally increased with decreasing DOC concentration, flow path, and stream order (Table 1). The TOC concentrations were on average 60% higher than the long-term averages due to the considerable rainfall prior to our sampling, which induced an increased flow of water through the organics-rich topsoil at all sites[8,38] (Table S1). Organic carbon >0.2 μm made up <3% of all samples (Table S3). This is in accordance with Laudon et al.,[34] who demonstrated that organic carbon >0.45 μm made up less than 0.6% of samples collected in all seasons throughout the entire catchment area.

The charge densities were between 4.0 and 8.6 μeq·mg_{DOC}^{-1} (Figure 1c). The wetland sites and the forested sites can be cleary distinguished as end members, with the wetland sites having the lowest charge densities (4.0−4.5 μeq·mg_{DOC}^{-1}) and the forested sites the highest charge densities (7.4−8.3 μeq·mg_{DOC}^{-1}) (Figure 1). This is in accordance with previously published data on charge densities from this catchment, which were low for the wetland sites even under varying flow conditions (4.6−5.0 μeq·mg_{TOC}^{-1}), while the other sites exhibited a larger variability (4.8−7.2 μeq·mg_{TOC}^{-1}) with lower values during acidic conditions at high flow.[39]

It is noticeable that the concentrations of functional groups varied only between 166 and 266 μeq·L^{-1}, even though the DOC concentrations varied by a factor of almost three (Figure 1). Humic acids contributed ≤13% to the DOC (Table S3), and the content of fulvic acids and small organic molecules was therefore 87 to 100%. The aromaticity of the samples, which was calculated from specific UV absorbance,[24] ranged from 29 to 35% (Table S3). The apparent molecular masses of the NOM, measured at the mode of the UV−vis peak (peak maximum) in the FlowFFF analyses, were between 2080 and 2650 g·mol^{-1} (Table S3, Figures S7−S11). The samples from the forested sites with a high content of fulvic acids and small organic molecules, and low apparent molecular mass, had a

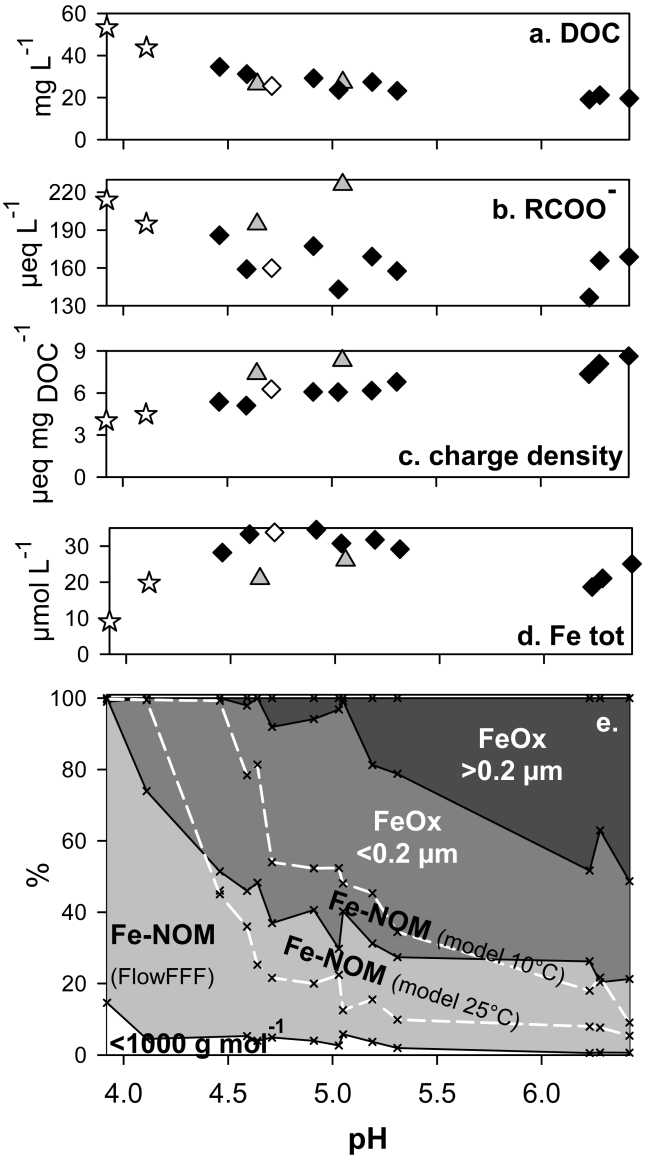

Figure 1. (a) DOC concentrations, (b) $RCOO^-$ concentrations, (c) charge densities of the DOC, and (d) total Fe concentrations (unfiltered), as a function of pH. The wetland sites are marked with stars, the forested sites with triangles, and the lake outlet with a white diamond. The other sites (shown as black diamonds) are in mixed catchments. (e) Fe percentages >0.2 μm, in the size range between 1000 g·mol^{-1} and 0.2 μm, associated with NOM (calculated from FlowFFF analysis), and passing through 1000 g·mol^{-1} membranes, all plotted as a function of pH. The percentage of Fe-NOM calculated from chemical equilibrium modeling at 10 and 25 °C is plotted as dashed white lines. The pool of Fe in the size range between 1000 g·mol^{-1} and 0.2 μm consists of both Fe-NOM and iron (oxy)-hydroxides (FeOx).

dx.doi.org/10.1021/es401193j | Environ. Sci. Technol. 2013, 47, 7120−7128

higher site density than the other samples (Table S3). This is in agreement with the increases in the total acidity and the contribution of carboxyl groups associated with decreasing molecular mass[40,41] and higher fulvic acid content, reported in the published literature.[42,43]

Variations in Fe Speciation with pH and Flow Path. The concentrations of Fe (total) ranged between 9 and 35 μmol·L^{-1} (Figure 1d), which is 2−3 orders of magnitude higher than the average world river.[3] The soils within the investigated catchment area are generally homogeneous with respect to mineralogy.[35] The Fe that ultimately reaches the streamwater derives mainly from the weathering of Fe-bearing minerals such as amphiboles, biotite, and chlorite.[35] However, wetland soils consist mainly of decomposing organic material that is poor in minerals,[22] which explains why Fe concentrations are lower at the acidic wetland sites (9.0 and 19.7 μmol·L^{-1}) than in the forested catchments (21 and 26 μmol·L^{-1}). The mixed sites had Fe concentrations that ranged between 28 and 35 μmol·L^{-1}, with slightly lower concentrations at those sites with pH >6 (19 to 25 μmol·L^{-1}). Inflows of Fe-rich groundwater, with total Fe concentrations of up to 350 μmol·L^{-1} in the catchments with a stream order >1, are the reason for the higher total Fe concentrations (19 to 35 μmol·L^{-1}) at the sites in mixed catchments than at the wetland and forested sites (Figure S2).

There was no more than 2% Fe(II) present in any of the samples except for site C4, which had 11% Fe(II) (Table S4). These low Fe(II) contents are in contrast to the results obtained by Lofts et al.,[44] who found that Fe(II) was an important component of dialysates from freshwater samples of different chemistries, making up 24% of the total Fe, on average. Between 0.5 and 15% of the Fe in our samples passed through the 1000 g·mol^{-1} ultrafiltration membranes (Figure 1e), except for one contaminated sample which was excluded (Table S4). The smallest fraction (<1000 g·mol^{-1}) is probably associated with low molecular mass NOM passing through the ultrafiltration membrane (3 to 5.9 mg·L^{-1} DOC), rather than truly dissolved Fe(III) because Fe(III) has a very low solubility.[44] The Fe <0.2 μm at the wetland sites was almost entirely complexed by NOM (Figure 1e), and the proportion of organically bound Fe decreased with increasing pH, and decreasing NOM concentrations down to approximately 20%. The pH-dependence of organically bound Fe is in accordance with results from freshwater samples collected in the UK, in which the proportion of organically complexed Fe(III) decreased from almost 100% at pH 4 to 10% or less at pH 7.[44,45]

Chemical equilibrium modeling using Visual MinteQ indicated that the water samples with pH >4.5 are supersaturated with respect to ferrihydrite (modeled at 10 and 25 °C; Table S4). The presence of iron (oxy)hydroxides was confirmed by SEM images with EDS analysis that identified particles containing Fe trapped on the 0.2 μm pore size membrane filter. The primary particle sizes were approximately 30−100 nm, forming aggregates of about 500 nm (Figure S12).

The modeled data for NOM-bound Fe showed the same pH trend as the FlowFFF data but were systematically higher or lower than the NOM-associated Fe concentrations measured by FlowFFF. This effect is due to the temperatures that were chosen for the modeling (10 °C or 25 °C, Figure 1e). The large differences from the modeled Fe-NOM concentrations were a result of variations with temperature in the solubility product of ferrihydrite (25 °C: log K_s = 2.67; 10 °C: log K_s = 3.61). The values at 10 °C, which is close to the streamwater temperature (9.4 ± 0.7 °C), apply to the filtrations that were undertaken with cooled samples. Cooled samples were used for the FlowFFF analysis, but during the analysis the sample equilibrated with the mobile FlowFFF phase (to ∼20 °C). Even though the FlowFFF derived Fe-NOM concentrations are closer to the concentrations modeled at 10 °C, variations can occur due to the formation of iron (oxy)hydroxides when the temperature changes, especially at low pH values.[46]

Other possible reasons for discrepancies between measured and modeled values are the use of generic binding parameters for NOM in the equilibrium model and losses of NOM and associated elements during the FlowFFF analysis.[26,47] The NOM recoveries (measured as UV−vis absorption) ranged between 63 and 77%, so that differences of about 30−40% could be related to the implied losses. In addition, the FlowFFF-method used in this study covered sizes from 1 nm to approximately 30 nm,[5,26] and thus the iron (oxy)hydroxides with sizes of 30−100 nm that were shown by SEM analysis are not captured by the analysis. This size range may, however, comprise significant assemblages of iron (oxy)hydroxides and NOM.[48] In addition, iron (oxy)hydroxides can also occur in the <10 nm size range and thus elute along with the NOM.[36]

Two Fe pools can be identified: Fe associated with NOM, which dominated at low pH sites, and iron (oxy)hydroxides that formed when the pH of the streamwater was >4.5 (Figure 1). Vasyukova et al.[12] proposed that a major process of formation for suspended iron (oxy)hydroxides in streams involved their precipitation at redox fronts in riparian zones. The groundwater in the riparian zones, which are located in the higher-order catchments, has a pH between 5.5 and 7.4, TOC concentrations <20 mg·L^{-1},[11] and total Fe concentrations as high as 350 μmol·L^{-1}. The TOC was recalculated to NOM in accordance with Lofts et al.[44] and Tipping et al.[45] by assuming that NOM comprises 50% organic carbon, and 65% of the NOM was assumed to be chemically active.[44] The Fe/NOM ratios in the riparian zones of the higher-order catchments ranged from 0.16 mmol·g_{NOM}^{-1} to 39 mmol·g_{NOM}^{-1} (Figure S2). Tipping et al.[45] reported that the Fe/NOM ratios at which the functional groups of NOM are saturated range from 0.001−0.8 mmol·g_{NOM}^{-1} and depend on the origin of the NOM, the pH, and competing cations such as Al. The NOM concentrations in the groundwater are therefore clearly not sufficient to complex all of the Fe. Fe may be present as Fe(II) in these soil waters or as small iron (oxy)hydroxides, depending on the redox conditions. The oxidation of Fe(II) bearing groundwater at the soil/water interface may therefore have contributed to a large extent to the precipitation of iron (oxy)hydroxides at the higher-order stream sites.

The riparian zones in the headwater catchments exhibit very high TOC concentrations (10−90 mg·L^{-1})[11] and lower Fe/NOM ratios than in the higher-order catchments. In the shallow layers that are the major contributors to solute export[11] the Fe/NOM ratios were <3 mmol·g_{NOM}^{-1} (Figure S2). This supports our finding that precipitation of iron (oxy)hydroxides is less important in the headwater catchments than in the higher-order catchments.

The size of the iron (oxy)hydroxide aggregates in the streamwater increased with increasing pH, with decreasing DOC, and with increasing stream order, eventually exceeding 0.2 μm (the pore size of the membrane filters) at the high pH downstream sites (Figure 1). Due to their large size, they are then prone to further aggregation and sedimentation. The low

total Fe concentrations (19 to 25 μmol·L^{-1}) in the streamwater near the catchment outlet compared to those in other mixed sites (28 to 35 μmol·L^{-1}) suggest a limited Fe mobility at the higher pH sites (pH >6) in the fourth-order streams. Nonfilterable Fe generally made up less than 50% of the total Fe, which is on average 50% lower than the observed long-term averages for nonfilterable Fe (Table S1, Figure S5).[22] At the same time, filterable Fe and DOC concentrations were 30 and 60% higher than the long-term averages, respectively (Table S1). This is probably due to the increased flow of water through the organic-rich topsoil at all sites due to the relatively wet conditions during sampling.[11] The lower concentrations of nonfilterable Fe under high flow conditions demonstrate the importance of hydrological flow conditions to NOM-associated Fe mobilization in boreal catchments.[1] The fraction of particulate Fe as a fucntion of pH in the September sampling was surprisingly close to the long-term average (Figure S5). The dependence of Fe speciation on the flow conditions has also been previously recognized in the large boreal catchment of the Kalix River.[49,50] However, while iron (oxy)hydroxide formation in the Kalix River occurs mainly during baseflow conditions,[49,50] our data set demonstrates that substantial amounts of Fe precipitate even under high flow conditions when pH is above 5 (Figure S5).

Iron Binding to NOM Compared to Other Studies. Previous studies have shown that, in freshwater, large quantities of Fe bind to NOM in equilibrium with iron (oxy)-hydroxides.[3,10,29,45,51−57] Figure 2 is a compilation of published

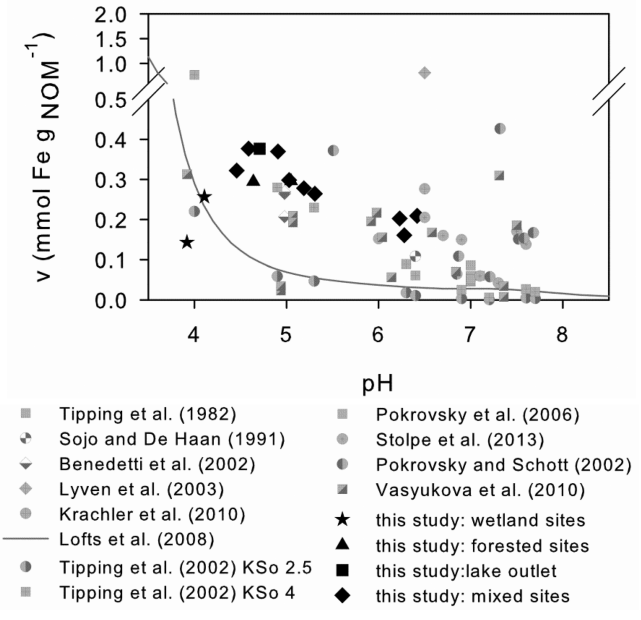

Figure 2. Fe loading values v from this study in comparison to loading values of freshwater samples from published literature.

data on Fe complexation by NOM, together with FlowFFF analysis data from this study. The millimoles of organically bound Fe per unit mass of active NOM (loading values) in equilibrium with iron (oxy)hydroxides were calculated in accordance with Lofts et al.[44] and Tipping et al.[45]

The loading values (v) were highest at the low pH mixed sites and decreased systematically with increasing pH (Figure 2). Even though almost all the Fe was bound to NOM at the wetland sites (Figure 1), the loading values were low. These samples contained only minor quantities of iron (oxy)-hydroxides (Figure 1), and the functional groups of the NOM were therefore probably not fully occupied with Fe.

The data from Lofts et al.[44] and Tipping et al., 2002[45] also exhibit a clear decrease in v with increasing pH (Figure 2). Loading values from this study are higher than the modeling-based values obtained by Tipping et al., 2002[45] using a solubility product (log K_s) of 2.5 and the modeled data by Lofts et al.[44] The values obtained by Lofts et al.[44] may be lower because they are based on dialysis (3500−15,000 g·mol^{-1}) of surface water samples, and not all the NOM (together with any complexed Fe) may have passed through the dialysis membranes. The values that we obtained from this study were close to the modeling results obtained by Tipping et al., 2002[45] when a log K_s value of 4 was used. This is in accordance with our finding that the Fe-NOM concentrations are best described using a high solubility product (log K_s = 3.61). Loading values derived by Sojo and De Haan[52] and Tipping et al., 1982[51] from centrifugation of lakewater were lower than our own results.

Benedetti et al.[10] reported that two colloidal fractions (5000 g·mol^{-1}−100,000 g·mol^{-1} and 100,000 g·mol^{-1}−0.2 μm) from the Rio Negro exhibited different loading values (Figure 2) and related the chemical differences between the two fractions to differences in their aromaticity. It is noticeable that the loading values were highest for those samples in our study that had a high specific UV absorbance and a high degree of aromaticity (Figure S4), in line with earlier experimental observations.[24] Stolpe et al., 2010[56] also related the high capacity for Fe complexation in some streams of the Mississippi river system to the high aromaticity of NOM (data not shown in Figure 2). The loading values for pH >6 in Figure 2 exhibit a wide variation, with the data by Lyven et al.[29] (using a FlowFFF technique similar to our own) being more than four times higher than our own data. The loading values from our study are twice as high as the data modeled by Tipping et al.[45] for pH >6, even when they used a solubility product of 4. Similarly, loading values calculated for other boreal surface water samples (FlowFFF analysis of Alaskan rivers samples, Stolpe et al., 2013[36] and ultrafiltration and dialysis (both 10,000 g·mol^{-1}) of surface water from Siberia and Russia, Vasyukova et al.,[12] Pokrovsky et al.,[37] and Pokrovsky and Schott[2]) are also relatively high for pH >6. This reveals the importance of Fe binding to NOM in this catchment and in general in boreal regions, even at relatively high pH values. The relevance of Fe-NOM complexes, even at neutral pH values, has already been demonstrated for synthetic samples,[13,19] with the authors concluding that organic complexes were sufficiently stable to suppress the precipitation of iron (oxy)hydroxides.[13,19]

There is growing interest in quantifying the fluxes of Fe in river systems and Fe transport to the oceans.[3,58] Fe complexed by NOM in streamwater has been shown to remain stable when it mixes with seawater[3,4] and thus could escape the estuarine mixing zone,[4] while iron (oxy)hydroxide colloids tend to aggregate. High concentrations of organically bound Fe have been observed in other boreal catchments such as that of the Kalix River,[49,50] indicating that boreal river systems are major contributors of Fe to the oceans. The amount of Fe reaching the ocean depends on the size of the iron (oxy)hydroxide particles.[4] The proportion of measured Fe >0.2 μm was much lower than the modeled amount of ferrihydrite (Table S4). Both the snapshot sampling and the long-term sampling indicate that Fe >0.2 μm occurs when the pH rises above 5.

dx.doi.org/10.1021/es401193j | Environ. Sci. Technol. 2013, 47, 7120−7128

About 50% of all Fe occurs in the >0.2 μm fraction in the higher-order catchments with a pH of 6, where more alkaline, Fe-rich groundwater enters the stream (Figure 2). Increasing DOC concentrations in the streamwater will thus lead to an increase in the mobilization of <0.2 μm Fe due to (a) an increased amount of Fe bound to NOM and (b) the suppression of iron (oxy)hydroxide formation.

As Association with NOM and Iron (Oxy)hydroxides. The concentrations of As in the streamwater ranged from 6.4 to 12.7 nmol·L^{-1}, but there was no clear correlation between these concentrations and either the source of the water or its pH (Figure 3). Dissolved As (<1000 g·mol^{-1}) predominated (30–60% of the total concentrations) over the As in the >0.2 μm fraction over the whole pH range. At the low-pH wetland sites, 70–75% of the As was in the size fraction between 1000 g·mol^{-1} and 0.2 μm (Figure 3). For higher pH values (from 4.3 to 5.2), between 30 and 55% of the As was in this size fraction, decreasing with increasing pH to between 26 and 38% at those sites with pH >6. When the pH was >4.5, up to 20% of the total As concentration was found in the >0.2 μm size fraction.

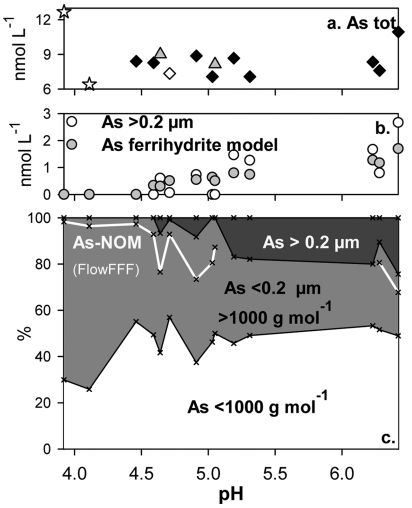

Figure 3. (a) Total As concentrations (unfiltered), plotted as a function of pH. The wetland sites are marked with stars, the forested sites with triangles, and the lake outlet with a white diamond. The other sites (shown as black diamonds) are in mixed catchments. (b) As concentrationa >0.2 μm and the modeled concentration of As sorbed to ferrihydrite. (c) As percentages >0.2 μm, in the size range between 1000 g·mol^{-1} and 0.2 μm, and passing through 1000 g·mol^{-1} membranes, all plotted as a function of pH. The association of As with NOM, as determined by FlowFFF, is presented as a white line. Note that in two of the samples the signal-to-noise ratio was too poor to allow the calculation of As-NOM concentrations.

Most of the As in the size fraction between 1000 g·mol^{-1} and 0.2 μm was associated with NOM (Figure 3). The signal-to-noise ratio in two of the samples was too low to allow the calculation of As-NOM concentrations (Figure S10). The percentage of As that we observed to be associated with NOM is higher than that previously observed by Buschmann et al.,[18] who found that only 10% of As was associated with NOM (DOC 5 mg·L^{-1}, pH 7, As(V) 67 nmol·L^{-1}). The difference between our figure and that observed by Buschmann et al.[18] could be due to the formation of As–Fe–NOM ternary complexes.[14,19,20] In our samples the moles of As per g of NOM associated with NOM (v, computed by analogy with Fe) ranged between $7.9\cdot10^{-8}$ and $1.5\cdot10^{-7}$ (Table S5). The proportion of As associated with NOM decreased with increasing pH (Figure 3). Buschmann et al.,[18] however, argued that if Fe bridges are important in As binding to NOM, the binding should increase at lower pH values due to the Fe speciation. When iron (oxy)hydroxides start to precipitate, the role of Fe bridging would be expected to decrease.[18] This is in accordance with our chemical equilibrium modeling, which revealed that the concentrations of As >0.2 μm could be explained by sorption of arsenate to ferrihydrite (Figure 3).

The modeled concentrations of arsenate bound to ferrihydrite are slightly lower than the measured concentrations of As >0.2 μm. However, a large pool of iron (oxy)hydroxides is present in the <0.2 μm size range. The concentrations of As associated with NOM are on average 20% lower than those of As in the size fraction between 1000 g·mol^{-1} and 0.2 μm (Figure 3, Table S5), which may be related to the sorption of As to iron (oxy)hydroxides within this size range.[55]

Our results highlight the importance of Fe-NOM interactions for the riverine transport of both Fe and As. The As-NOM complexes were important for As speciation under the investigated conditions (high NOM concentrations and low pH). The association of As with iron (oxy)hydroxides at pH >4.5 couples its transport to that of the iron (oxy)hydroxides.

Environmental Implications. The results from this study reveal that the speciation of Fe and As can vary considerably during the passage from wetland-dominated headwaters to less acidic higher-order streams. Fe-NOM complexes were dominant at the low pH sites, but inflows of Fe-rich groundwater and increases in pH in the higher-order streams induced precipitation of iron (oxy)hydroxides. Separating organic and inorganic forms of Fe remains analytically challenging in transient systems; the observed congruence between Fe-NOM binding patterns derived from FlowFFF analysis and the patterns from modeled data indicates that FlowFFF-ICP-MS is well suited for studying trace element speciation, even in these complex samples.

Iron (oxy)hydroxides act as carriers for a large number of (toxic) metals and metalloids, and agglomerates may eventually settle in slow-flowing stream sections thus removing these metals, at least temporarily, from the aqueous phase. These deposits may, however, be remobilized during stormwater flow.

The high concentrations of organically bound Fe in our samples and in surface water samples from other boreal regions, compared to those in other published data and the long-term averages, emphasize the importance of boreal catchments in riverine export of Fe into oceans and of Fe-NOM associations during high flow conditions.

■ ASSOCIATED CONTENT

Ⓢ Supporting Information

Information on physical and chemical characteristics of the catchment, NOM analyses data, Fe and As speciation data, details on the FlowFFF analysis and scanning electron microscopy image; Figures S1–S12, and Tables S1–S5. This material is available free of charge via the Internet at http://pubs.acs.org.

■ AUTHOR INFORMATION

Corresponding Author

*Phone: + 43 1 4277 53320. Fax: + 43 1 4277 9533. E-mail: thilo.hofmann@univie.ac.at (T.H.). Phone: +43-1-4277-53380. Fax: + 43 1 4277 9533. E-mail: frank.kammer@univie.ac.at (F.v.d.K.).

Notes

The authors declare no competing financial interest.

■ ACKNOWLEDGMENTS

This study was funded by the University of Vienna, the Swedish Research Council Formas (ForWater Project), Future Forest, the Swedish Nuclear Fuel and Waste Management Company (SKB), and the Kempe Foundation, within the framework of the Krycklan Catchment Study. Particular thanks go to Ida Taberman (Swedish University of Agricultural Sciences) for help with field work and technical support in the laboratory, to José L. J. Ledesma for provision of the maps of the catchments, and to Wolfgang Obermaier and Gerlinde Habler (University of Vienna) for support with ICP-OES and ICP-MS measurements and electron microscope imaging.

■ REFERENCES

(1) Erlandsson, M.; Buffam, I.; Fölster, J.; Laudon, H.; Temnerud, J.; Weyhenmeyer, G. A.; Bishop, K. Thirty-five years of synchrony in the organic matter concentrations of Swedish rivers explained by variation in flow and sulphate. *Glob. Change Biol.* **2008**, *14* (5), 1191−1198.

(2) Pokrovsky, O. S.; Schott, J. Iron colloids/organic matter associated transport of major and trace elements in small boreal rivers and their estuaries (NW Russia). *Chem. Geol.* **2002**, *190* (1−4), 141−179.

(3) Krachler, R.; Krachler, R. F.; von der Kammer, F.; Süphandag, A.; Jirsa, F.; Ayromlou, S.; Hofmann, T.; Keppler, B. K. Relevance of peat-draining rivers for the riverine input of dissolved iron into the ocean. *Sci. Total Environ.* **2010**, *408* (11), 2402−2408.

(4) Stolpe, B.; Hassellöv, M. Changes in size distribution of fresh water nanoscale colloidal matter and associated elements on mixing with seawater. *Geochim. Cosmochim. Acta* **2007**, *71* (13), 3292−3301.

(5) Neubauer, E.; von der Kammer, F.; Hofmann, T. Using FlowFFF and HPSEC to determine trace metal-colloid associations in wetland runoff. *Water Res.* **2013**, *47* (8), 2757−2769.

(6) Monteith, D. T.; Stoddard, J. L.; Evans, C. D.; De Wit, H. A.; Forsius, M.; Høgåsen, T.; Wilander, A.; Skjelkvåle, B. L.; Jeffries, D. S.; Vuorenmaa, J.; Keller, B.; Kopécek, J.; Vesely, J. Dissolved organic carbon trends resulting from changes in atmospheric deposition chemistry. *Nature* **2007**, *450* (7169), 537−540.

(7) Kritzberg, E. S.; Ekström, S. M. Increasing iron concentrations in surface waters - a factor behind brownification? *Biogeosciences* **2012**, *9* (4), 1465−1478.

(8) Buffam, I.; Laudon, H.; Seibert, J.; Mörth, C.-M.; Bishop, K. Spatial heterogeneity of the spring flood acid pulse in a boreal stream network. *Sci. Total Environ.* **2008**, *407* (1), 708−722.

(9) Hruška, J.; Köhler, S.; Laudon, H.; Bishop, K. Is a universal model of organic acidity possible: Comparison of the acid/base properties of dissolved organic carbon in the boreal and temperate zones. *Environ. Sci. Technol.* **2003**, *37* (9), 1726−1730.

(10) Benedetti, M.; Ranville, J. F.; Ponthieu, M.; Pinheiro, J. P. Field-flow fractionation characterization and binding properties of particulate and colloidal organic matter from the Rio Amazon and Rio Negro. *Org. Geochem.* **2002**, *33* (3), 269−279.

(11) Grabs, T.; Bishop, K.; Laudon, H.; Lyon, S. W.; Seibert, J. Riparian zone hydrology and soil water total organic carbon (TOC): implications for spatial variability and upscaling of lateral riparian TOC exports. *Biogeosciences* **2012**, *9* (10), 3901−3916.

(12) Vasyukova, E. V.; Pokrovsky, O. S.; Viers, J.; Oliva, P.; Dupré, B.; Martin, F.; Candaudap, F. Trace elements in organic- and iron-rich surficial fluids of the boreal zone: Assessing colloidal forms via dialysis and ultrafiltration. *Geochim. Cosmochim. Acta* **2010**, *74* (2), 449−468.

(13) Karlsson, T.; Persson, P. Complexes with aquatic organic matter suppress hydrolysis and precipitation of Fe(III). *Chem. Geol.* **2012**, *322*−*323*, 19−27.

(14) Redman, A. D.; Macalady, D. L.; Ahmann, D. Natural organic matter affects arsenic speciation and sorption onto hematite. *Environ. Sci. Technol.* **2002**, *36* (13), 2889−2896.

(15) Sharma, P.; Ofner, J.; Kappler, A. Formation of binary and ternary colloids and dissolved complexes of organic matter, Fe and As. *Environ. Sci. Technol.* **2010**, *44* (12), 4479−4485.

(16) Plathe, K. L.; von der Kammer, F.; Hassellöv, M.; Moore, J. N.; Murayama, M.; Hofmann, T.; Hochella, M. F., Jr. The role of nanominerals and mineral nanoparticles in the transport of toxic trace metals: Field-flow fractionation and analytical TEM analyses after nanoparticle isolation and density separation. *Geochim. Cosmochim. Acta* **2013**, *102* (0), 213−225.

(17) Warwick, P.; Inam, E.; Evans, N. Arsenic's interaction with humic acid. *Environ. Chem.* **2005**, *2* (2), 119−124.

(18) Buschmann, J.; Kappeler, A.; Lindauer, U.; Kistler, D.; Berg, M.; Sigg, L. Arsenite and arsenate binding to dissolved humic acids: Influence of pH, type of humic acid, and aluminum. *Environ. Sci. Technol.* **2006**, *40* (19), 6015−6020.

(19) Mikutta, C.; Kretzschmar, R. Spectroscopic evidence for ternary complex formation between arsenate and ferric iron complexes of humic substances. *Environ. Sci. Technol.* **2011**, *45* (22), 9550−9557.

(20) Ritter, K.; Aiken, G. R.; Ranville, J. F.; Bauer, M.; Macalady, D. L. Evidence for the aquatic binding of arsenate by natural organic matter−suspended Fe(III). *Environ. Sci. Technol.* **2006**, *40* (17), 5380−5387.

(21) Buffam, I.; Laudon, H.; Temnerud, J.; Mörth, C. M.; Bishop, K. Landscape-scale variability of acidity and dissolved organic carbon during spring flood in a boreal stream network. *J. Geophys. Res.: Biogeosci.* **2007**, *112* (1), G01022.

(22) Björkvald, L.; Buffam, I.; Laudon, H.; Mörth, C.-M. Hydrogeochemistry of Fe and Mn in small boreal streams: The role of seasonality, landscape type and scale. *Geochim. Cosmochim. Acta* **2008**, *72* (12), 2789−2804.

(23) Stookey, L. L. Ferrozine - a new spectrophotometric reagent for iron. *Anal. Chem.* **1970**, *42* (7), 779−781.

(24) Weishaar, J. L.; Aiken, G. R.; Bergamaschi, B. A.; Fram, M. S.; Fujii, R.; Mopper, K. Evaluation of specific ultraviolet absorbance as an indicator of the chemical composition and reactivity of dissolved organic carbon. *Environ. Sci. Technol.* **2003**, *37* (20), 4702−4708.

(25) Stevenson, F. J. *Humus chemistry - Genesis, Composition, Reactions*; John Wiley and Sons, Inc.: 1994.

(26) Neubauer, E.; von der Kammer, F.; Hofmann, T. Influence of carrier solution ionic strength and injected sample load on retention and recovery of natural nanoparticles using flow field-flow fractionation. *J. Chromatogr., A* **2011**, *1218* (38), 6763−6773.

(27) Hassellöv, M.; von der Kammer, F.; Beckett, R. Characterisation of Aquatic Colloids and Macromolecules by Field-Flow Fractionation. In *Environmental colloids and particles: behaviour, separation, and characterisation*; Wilkinson, K. J., Lead, J. R., Eds.; John Wiley & Sons Ltd.: Chichester, 2007.

(28) Neubauer, E.; Schenkeveld, W. D. C.; Plathe, K. L.; Rentenberger, C.; von der Kammer, F.; Kraemer, S. M.; Hofmann, T. The influence of pH on iron speciation in podzol extracts: iron complexes with natural organic matter, and iron mineral nanoparticles. *Sci. Total Environ.* DOI 10.1016/j.scitotenv.2013.04.076

(29) Lyvén, B.; Hassellöv, M.; Turner, D. R.; Haraldsson, C.; Andersson, K. Competition between iron- and carbon-based colloidal carriers for trace metals in a freshwater assessed using flow field-flow fractionation coupled to ICPMS. *Geochim. Cosmochim. Acta* **2003**, *67* (20), 3791−3802.

(30) Baalousha, M.; Stolpe, B.; Lead, J. R. Flow field-flow fractionation for the analysis and characterization of natural colloids and manufactured nanoparticles in environmental systems: A critical review. *J. Chromatogr., A* **2011**, *1218* (27), 4078−4103.

(31) Sjöstedt, C. S.; Gustafsson, J. P.; Köhler, S. J. Chemical equilibrium modeling of organic acids, pH, aluminum, and iron in Swedish surface waters. *Environ. Sci. Technol.* **2010**, *44* (22), 8587−8593.

(32) Gustafsson, J. P. Modeling the acid-base properties and metal complexation of humic substances with the Stockholm Humic Model. *J. Colloid Interface Sci.* **2001**, *244* (1), 102−112.
(33) Dzombak, D.; Morel, F. M. M. *Surface complexation modeling: Hydrous ferric oxide*; Wiley: New York, 1990.
(34) Laudon, H.; Berggren, M.; Agren, A.; Buffam, I.; Bishop, K.; Grabs, T.; Jansson, M.; Köhler, S. Patterns and dynamics of dissolved organic carbon (DOC) in boreal streams: The role of processes, connectivity, and scaling. *Ecosystems* **2011**, *14*, 880−893.
(35) Ledesma, J. L. J.; Grabs, T.; Futter, M. N.; Bishop, K. H.; Laudon, H.; Köhler, S. J. Riparian zone controls on base cation concentrations in boreal streams. *Biogeosciences Discuss.* **2013**, *10* (1), 739−785.
(36) Stolpe, B.; Guo, L.; Shiller, A. M.; Aiken, G. R. Abundance, size distributions and trace-element binding of organic and iron-rich nanocolloids in Alaskan rivers, as revealed by field-flow fractionation and ICP-MS. *Geochim. Cosmochim. Acta* **2013**, *105* (0), 221−239.
(37) Pokrovsky, O. S.; Schott, J.; Dupré, B. Trace element fractionation and transport in boreal rivers and soil porewaters of permafrost-dominated basaltic terrain in Central Siberia. *Geochim. Cosmochim. Acta* **2006**, *70* (13), 3239−3260.
(38) Köhler, S. J.; Buffam, I.; Laudon, H.; Bishop, K. H. Climate's control of intra-annual and interannual variability of total organic carbon concentration and flux in two contrasting boreal landscape elements. *J. Geophys. Res.: Biogeosci.* **2008**, *113* (3), G03012.
(39) Hruška, J.; Laudon, H.; Johnson, C. E.; Köhler, S.; Bishop, K. Acid/base character of organic acids in a boreal stream during snowmelt. *Water Resour. Res.* **2001**, *37* (4), 1043−1056.
(40) Fukushima, M.; Tanaka, S.; Nakamura, H.; Ito, S. Acid-base characterization of molecular weight fractionated humic acid. *Talanta* **1996**, *43* (3), 383−390.
(41) Christl, I.; Kretzschmar, R. Relating ion binding by fulvic and humic acids to chemical composition and molecular size. 1. Proton binding. *Environ. Sci. Technol.* **2001**, *35* (12), 2505−2511.
(42) Bratskaya, S.; Golikov, A.; Lutsenko, T.; Nesterova, O.; Dudarchik, V. Charge characteristics of humic and fulvic acids: Comparative analysis by colloid titration and potentiometric titration with continuous pK-distribution function model. *Chemosphere* **2008**, *73* (4), 557−563.
(43) Gondar, D.; Lopez, R.; Fiol, S.; Antelo, J. M.; Arce, F. Characterization and acid−base properties of fulvic and humic acids isolated from two horizons of an ombrotrophic peat bog. *Geoderma* **2005**, *126* (3−4), 367−374.
(44) Lofts, S.; Tipping, E.; Hamilton-Taylor, J. The chemical speciation of Fe(III) in freshwaters. *Aquat. Geochem.* **2008**, *14* (4), 337−358.
(45) Tipping, E.; Rey-Castro, C.; Bryan, S. E.; Hamilton-Taylor, J. Al(III) and Fe(III) binding by humic substances in freshwaters, and implications for trace metal speciation. *Geochim. Cosmochim. Acta* **2002**, *66* (18), 3211−3224.
(46) Liu, X.; Millero, F. J. The solubility of iron hydroxide in sodium chloride solutions. *Geochim. Cosmochim. Acta* **1999**, *63* (19−20), 3487−3497.
(47) Ulrich, A.; Losert, S.; Bendixen, N.; Al-Kattan, A.; Hagendorfer, H.; Nowack, B.; Adlhart, C.; Ebert, J.; Lattuada, M.; Hungerbühler, K. Critical aspects of sample handling for direct nanoparticle analysis and analytical challenges using asymmetric field flow fractionation in a multi-detector approach. *J. Anal. At. Spectrom.* **2012**, *27* (7), 1120−1130.
(48) Pokrovsky, O. S.; Shirokova, L. S.; Kirpotin, S. N.; Audry, S.; Viers, J.; Dupré, B. Effect of permafrost thawing on organic carbon and trace element colloidal speciation in the thermokarst lakes of western Siberia. *Biogeosciences* **2011**, *8* (3), 565−583.
(49) Ingri, J.; Malinovsky, D.; Rodushkin, I.; Baxter, D. C.; Widerlund, A.; Andersson, P.; Gustafsson, O.; Forsling, W.; Öhlander, B. Iron isotope fractionation in river colloidal matter. *Earth Planet. Sci. Lett.* **2006**, *245* (3−4), 792−798.
(50) Dahlqvist, R.; Andersson, K.; Ingri, J.; Larsson, T.; Stolpe, B.; Turner, D. Temporal variations of colloidal carrier phases and associated trace elements in a boreal river. *Geochim. Cosmochim. Acta* **2007**, *71* (22), 5339−5354.
(51) Tipping, E.; Woof, C.; Ohnstad, M. Forms of iron in the oxygenated waters of Esthwaite Water, U.K. *Hydrobiologia* **1982**, *91*−*92* (0), 383−393.
(52) Sojo, L. E.; De Haan, H. Multicomponent kinetic analysis of iron speciation in Humic lake Tjeukemeer: Comparison of fulvic acid from the drainage basin and lake water samples. *Environ. Sci. Technol.* **1991**, *25* (5), 935−939.
(53) Warnken, K. W.; Lawlor, A. J.; Lofts, S.; Tipping, E.; Davison, W.; Zhang, H. In situ speciation measurements of trace metals in headwater streams. *Environ. Sci. Technol.* **2009**, *43* (19), 7230−7236.
(54) Benedetti, M. F.; Ranville, J. F.; Allard, T.; Bednar, A. J.; Menguy, N. The iron status in colloidal matter from the Rio Negro, Brasil. *Colloids Surf., A* **2003**, *217* (1−3), 1−9.
(55) Stolpe, B.; Hassellöv, M.; Andersson, K.; Turner, D. R. High resolution ICPMS as an on-line detector for flow field-flow fractionation; multi-element determination of colloidal size distributions in a natural water sample. *Anal. Chim. Acta* **2005**, *535* (1−2), 109−121.
(56) Stolpe, B.; Guo, L.; Shiller, A. M.; Hassellöv, M. Size and composition of colloidal organic matter and trace elements in the Mississippi River, Pearl River and the northern Gulf of Mexico, as characterized by flow field-flow fractionation. *Mar. Chem.* **2010**, *118* (3−4), 119−128.
(57) Baalousha, M.; von der Kammer, F.; Motelica-Heino, M.; Baborowski, M.; Hofmeister, C.; Le Coustumer, P. Size-based speciation of natural colloidal particles by flow field flow fractionation, inductively coupled plasma-mass spectroscopy, and transmission electron microscopy/X-ray energy dispersive spectroscopy: Colloids-trace element interaction. *Environ. Sci. Technol.* **2006**, *40* (7), 2156−2162.
(58) Jirsa, F.; Neubauer, E.; Kittinger, R.; Hofmann, T.; Krachler, R.; von der Kammer, F.; Keppler, B. K. Natural organic matter and iron export from the Tanner Moor, Austria. *Limnologica* **2013**, *43*, 239−244.